MOLECULAR AND CELLULAR BIOLOGY, Aug. 2001, p. 5658–5666 Vol. 21, No. 16
0270-7306/01/$04.00+0 DOI: 10.1128/MCB.21.16.5658–5666.2001


# Gene Targeting Reveals a Crucial Role for *MTG8* in the Gut

FRANCO CALABI,[1]* RICHARD PANNELL,[2] AND GORDANA PAVLOSKA[1]

*Institute of Child Health, London WCIN 1EH,[1] and MRC Laboratory of Molecular Biology, Cambridge CB2 2QH,[2] United Kingdom*

Received 7 February 2001/Returned for modification 2 April 2001/Accepted 23 May 2001

**The *MTG8* (*ETO*) locus is involved in a reciprocal exchange with *runx1* in the t(8;21) of acute myeloid leukemia. It is a member of a small gene family encoding transcriptional regulators that interact with corepressors and histone deacetylase. However, the physiologic cellular processes controlled by *MTG8* are not known. In order to gain an insight into the latter, we have generated mutant mice with an insertional inactivation at the locus, which disrupts transcription of exon 2. The postnatal viability of homozygous mutants was greatly reduced. In approximately 25% the midgut was missing, whereas practically all pups surviving past the first 2 days showed severe growth impairment, which was likely due to a gross disruption of the gut architecture. The latter phenotype could be traced back to late embryonic development. No difference in gut cell differentiation or proliferation was found compared to wild-type littermates. Levels of factors known to be involved in gut morphogenesis were also unchanged. *MTG8* is expressed in the outermost layers of the developing gut from at least E9.5. Thus, *MTG8* plays a novel, essential role in the gastrointestinal system.**

The study of tumor-associated chromosomal translocations has led to the identification of genes that play a key role in controlling cell growth and differentiation (26). In the t(8;21) of acute myeloid leukemia (AML), early work showed the breakpoints to fall within the coding sequence of two previously unknown genes, *runx1* at 21q22 (previously named *AML1*/*CBFA2*) (21) and *MTG8* at 8q22 (also named *ETO*/*CDR*) (20). The former is related to the *runt* gene of *Drosophila melanogaster* and, together with it, defines a novel family of DNA-binding transcription factors (14, 33). Mouse *runx1* has been shown to be essential for definitive hemopoiesis (23, 37) and haploinsufficiency at *runx1* in humans is associated with diserythropoiesis and an increased risk of AML (32). Another *runx* member (*runx2*) is essential for osteogenesis in mammals, as shown both by gene targeting (16, 24) and by its mutations in cases of human cleidocranial dysplasia (22).

Relatively little is known about *MTG8*/*ETO*. It belongs to a small, phylogenetically conserved family, consisting of three members in humans and mice (4, 7, 10, 15) and one member in *D. melanogaster* (9). The latter (*nervy*) was identified as a target of the homeotic gene *Ubx*, and its expression in embryogenesis is largely restricted to precursors of the central and peripheral nervous system. However, there is no known phenotype associated with its mutations. Sequence comparison has identified four regions conserved among all MTG8-like polypeptides (4, 15). The COOH-terminal of these (NHR4, for nervy homology region 4) has the potential to fold as a double zinc finger, although it does not bind DNA (F. Calabi, unpublished results). The most $NH_2$-proximal region (NHR1) is related to $TAF_{II}$, a class of molecules involved in transcription initiation by RNA polymerase II (1). The notion that *MTG8* is implicated in gene transcription is strengthened by two additional observations: first, MTG8 products are primarily localized to the nucleus (7, 8, 18) and, second, they interact with corepressors such as N-CoR and mSin3, leading to the recruitment of histone deacetylase to the transcription complex (11, 19, 36). Based on Northern blotting analysis, *MTG8* in the adult is expressed mainly in the central nervous system, lungs, heart, and testis (20, 40). However, the cellular functions in which *MTG8* is involved are not known.

In order to gain an insight into the latter, we have introduced a targeted mutation at the mouse *MTG8* locus. Its phenotype reveals a crucial role in the gastrointestinal system.

## MATERIALS AND METHODS

**Gene targeting.** A mouse genomic library from strain 129/Sv in phage λ2001 (38) was screened with an *MTG8* probe spanning exons 2 to 4 (Table 1). Two overlapping clones (λESMM5 and λESMM9) were chosen for further manipulations. A targeting vector was assembled in pUC18, by subcloning an ~1.5-kb partial *Bgl*II/*Sst*I fragment from λESMM5 spanning most of exon 2, and an ~7-kb *Sst*I fragment from λESMM9 spanning exon 3. An *Escherichia coli lacZ* gene (from the *Kpn*I site at nucleotide (nt) 624 to the *Xba*I site at nt 4158 in plasmid pSV–β-galactosidase [Promega]) was inserted, after blunting, at the internal *Sst*I site, giving an in-frame fusion to exon 2. A 1.1-kb fragment encoding the *neo*$^r$ gene (from a modified pMC1neo PolyA vector [34]) was inserted at the *Bam*HI site at the 3′ end of the *lacZ* gene, and a 2-kb fragment encoding the herpes simplex virus *tk* gene (38) was inserted at the 3′ end of the mouse sequence (with respect to the *MTG8* transcriptional orientation).

The *Sal*I-linearized vector was transfected into CCB ES cells by electroporation as previously described (38). G418 and gangciclovir double-resistant clones were screened by Southern blotting using a 5′ flanking probe (a 0.3-kb *Pst*I fragment, mapping ~1.5 kb upstream of the region used to assemble the vector; Fig. 1A). Clones giving the expected pattern were further analyzed using a 3′ probe (a 0.6-kb *Rsa*I/*Xba*I fragment mapping ~5-kb downstream of the region used to assemble the vector; Fig. 1A) and a *neo* probe (the whole 1.1-kb fragment used for vector construction) to confirm single integration. Two clones were injected into C57BL/6 blastocysts, one of which (MTG8-lacZ222) yielded a high degree of chimerism and germ line transmission. Chimeras were backcrossed to C57BL/6, and further generations were produced by interbreeding.

**Histological analysis.** Organ samples were removed immediately following sacrifice and fixed either in buffered formalin or in Bouin's solution overnight at room temperature, prior to embedding in paraffin and sectioning at 4 to 6 μm.

Staining with hematoxylin and eosin, or Alcian blue was performed according to standard protocols. For immunohistochemistry, the following monoclonal antibodies were used as primary reagents: anti-PCNA (clone sc-56 [Santa Cruz Biotechnology], 1 μg/ml), anti-human sucrase-isomaltase (clone MGlu2 [12], culture supernatant diluted 1:64), anti-α smooth muscle actin (clone 1A4 [Sig-

* Corresponding author. Mailing address: Developmental Biology Unit, The Institute of Child Health, 30 Guilford St., London WCIN 1EH, United Kingdom. Phone: 44-20-7813-8492. Fax: 44-20-7831-4366. E-mail: fcalabi@hgmp.mrc.ac.uk.

TABLE 1. Probes used in the present study

| Locus | GenBank accession no. | 5′ end nt | 3′ end nt | Length (nt) |
|---|---|---|---|---|
| *Actin* | X03765 | 74 | 178 | 105 |
| *Bmp2* | L25602 | 8168 | 8363 | 196 |
| *Bmp4* | D14814 | 8453 | 8700 | 248 |
| *Cdx1* | M80463 | 5939 | 6132 | 194 |
| *Cdx2* | MM454 | 6244 | 6495 | 252 |
| *Fkh6* | X92498 | 939 | 1246 | 308 |
| *Nkx2-3* | AF155583 | 667 | 919 | 253 |
| *MTG8* | D14821 | 275 | 667 | 393 |

ma], ascitic fluid diluted 1:800), and anti-β tubulin III (clone SDL.3D10 [Sigma], ascitic fluid diluted 1:1,600). A biotinylated horse anti-mouse immunoglobulin G (Vector Laboratories, 7.5 μg/ml) was used as a secondary reagent. Biotinylated *Ulex europaeus* agglutinin I (UEAI) lectin was purchased from Vector Laboratories and used at 7.5 μg/ml. Sections were deparaffinized, rehydrated, treated with 3% $H_2O_2$ in methanol for 10 min, heated to 95°C in a microwave oven for 10 min, and blocked in 10% horse serum in phosphate-buffered saline (PBS) for 30 min. Antibodies were diluted in 10% horse serum in PBS and incubated for 30 to 60 min at room temperature. The results were visualized with the Vectastain Elite kit (Vector Laboratories), using diaminobenzidine as the substrate, following the manufacturer's instructions. Sections were lightly counterstained with Gill's hematoxylin.

Embryos were fixed in 4% paraformaldehyde in PBS for 3 to 12 h and stained with X-Gal (5-bromo-4-chloro-3-indolyl-β-D-galactopyranoside) according to a published protocol (29) prior to embedding and sectioning as described above. Sections were counterstained with eosin.

**RNA analysis.** Total RNA was extracted from fresh tissues by the guanidine-acid phenol method (6). For gene expression studies, probes (Table 1) were prepared by PCR amplification from mouse genomic DNA, cloned in M13 phage, and sequenced to confirm their identity.

High-specific activity, single-stranded DNA probes were prepared according to standard procedures (28). Ca. $5 \times 10^4$ cpm were mixed with ~20 μg of total RNA in 20 μl of 50% formamide–0.5 M NaCl–1 mM $Na_2EDTA$–25 mM PIPES (pH 6.8), heated at 50°C for 30 min, and then left to hybridize at 45°C for ~18 h. S1 digestion was with 25 U for 30 min at 37°C.

**Western blotting analysis.** Tissue extracts were prepared by homogenizing fresh organs in 10 volumes of 10% sodium dodecyl sulfate (SDS)–10 mM EDTA–25 mM Tris-Cl (pH 6.8) using an Ultra-Turrax homogenizer (IKA). Approximately 150 μg of total protein was fractionated by SDS-polyacrylamide gel electrophoresis on 7.5% gels and electroblotted onto polyvinylidene difluoride membranes (Hybond-P; Amersham Pharmacia Biotech) in 192 mM glycine–25 mM Tris–20% methanol at 125 V for 2 h. Blots were probed with a rabbit polyclonal antiserum raised against the C-terminal 212 amino acids of MTG8 (PC283; Oncogene Research Products; final concentration, 2.5 μg/ml), followed by horseradish peroxidase-coupled anti-rabbit antiserum (Amersham Pharmacia Biotech; 1:40,000), and developed using the ECL-Plus system (Amersham Pharmacia Biotech).

## RESULTS

**Gene targeting of mouse *MTG8*.** The human *MTG8* locus consists of at least 13 exons spanning >87 kb (40; F.C., unpublished). We chose to target exon 2, since it represents the common splice acceptor for a number of alternative upstream exons (20; F. Calabi, unpublished data), and it is the exon to which 5′ *runx1* sequences are most frequently spliced in transcripts deriving from the t(8;21) (30, 35).

Mouse genomic clones containing *MTG8* exons 2 and 3 were isolated from an 129/Sv library. An *E. coli lacZ* coding sequence was inserted in frame in place of the 3′ end of exon 2 and of the adjoining intron, in order simultaneously to disrupt *MTG8* transcription and to enable tracking of exon 2 expression by assaying for β-galactosidase activity. *neo*$^r$ and *tk* cassettes were further inserted in order to allow selection of homologous recombinants according to a standard strategy. The structure of the resulting targeted allele, *MTG8*$^{Ex2/lacZ}$, is illustrated in Fig. 1A.

Following electroporation in CCB ES cells, screening of 230 G418 plus gangciclovir double resistant clones by Southern blotting yielded three homologous recombinants. Only one, however, gave chimeras when injected into C57BL/6 blastocysts. Detailed genomic analysis of this clone by Southern blotting with probes flanking either end of the targeting vector, as well as for the inserted *neo*$^r$ gene (Fig. 1B), confirmed correct and unique integration of the mutation.

The effect of the introduced mutation on *MTG8* expression was investigated both at the RNA and at the protein level in extracts from brain, where the highest levels of MTG8 mRNA are found (20, 40). In nuclease protection experiments with a cDNA probe, a protected fragment corresponding to spliced exons 2 to 4 and representing the major species in the wild type (wt) is completely absent in the mutant (Fig. 1C). However, a fragment corresponding to alternative splicing upstream of exon 3, which is barely visible in the wt, is substantially increased in the mutant. Consistent with this result, a 3′ untranslated region (UTR) probe gives a comparable signal in both the mutant and the wt (data not shown).

On Western blotting analysis with an antiserum directed against the C-terminal domain of MTG8, two species of ca. 75 and 90 kDa are absent in the mutant, whereas a smaller species of ca. 55 kDa is increased, and a much larger polypeptide of >200 kDa is unchanged (Fig. 1D). The size of the two former polypeptides is consistent with that reported in human cell lines (8), whereas the other species must either result from alternative splicing or correspond to cross-reacting MTG8 paralogues. Altogether, the data confirm that the *MTG8*$^{Ex2/lacZ}$ mutation prevents the synthesis of wt MTG8 products carrying exon 2-encoded sequences.

**Reduced viability of *MTG8* exon 2-targeted mice.** The viability and fertility of *MTG8*$^{Ex2/lacZ}$ heterozygous mice were essentially identical to those of wt controls. Upon mating, heterozygous mice gave birth to the three expected genotypes in Mendelian ratios. However, postnatal viability of homozygous mutant pups was greatly reduced (Fig. 2A). Moreover, nearly all of those that survived past the first 2 days showed significantly reduced size and usually died before reaching puberty. Of the few adults, females were fertile, despite the reduced size, while no progeny were ever obtained from the males, despite successful mating, as judged by the formation of a vaginal plug.

**Absence of the midgut in *MTG8* exon 2-targeted mice.** While there was no significant difference in size and general appearance among $P_0/P_1$ pups born of heterozygous crosses, a fraction showed a distinctive pallor and no milk in their stomach. Upon sacrifice, these pups revealed a striking phenotype, consisting in the absence of most of the intestine, spanning from the distal duodenum to the greater part of the colon (Fig. 2B). The missing segments largely correspond to the districts supplied by the superior mesenteric artery, i.e., the midgut. On this basis, we operationally refer to this phenotype as Δmidgut (i.e., deletion of the midgut). It was never observed past $P_1$, likely causing early postnatal death.

Of the residual intestinal segments, the proximal (duodenal) stump was pervious and showed an outgrowth of the mucosa, with villi projecting into the peritoneal cavity. The distal (rec-

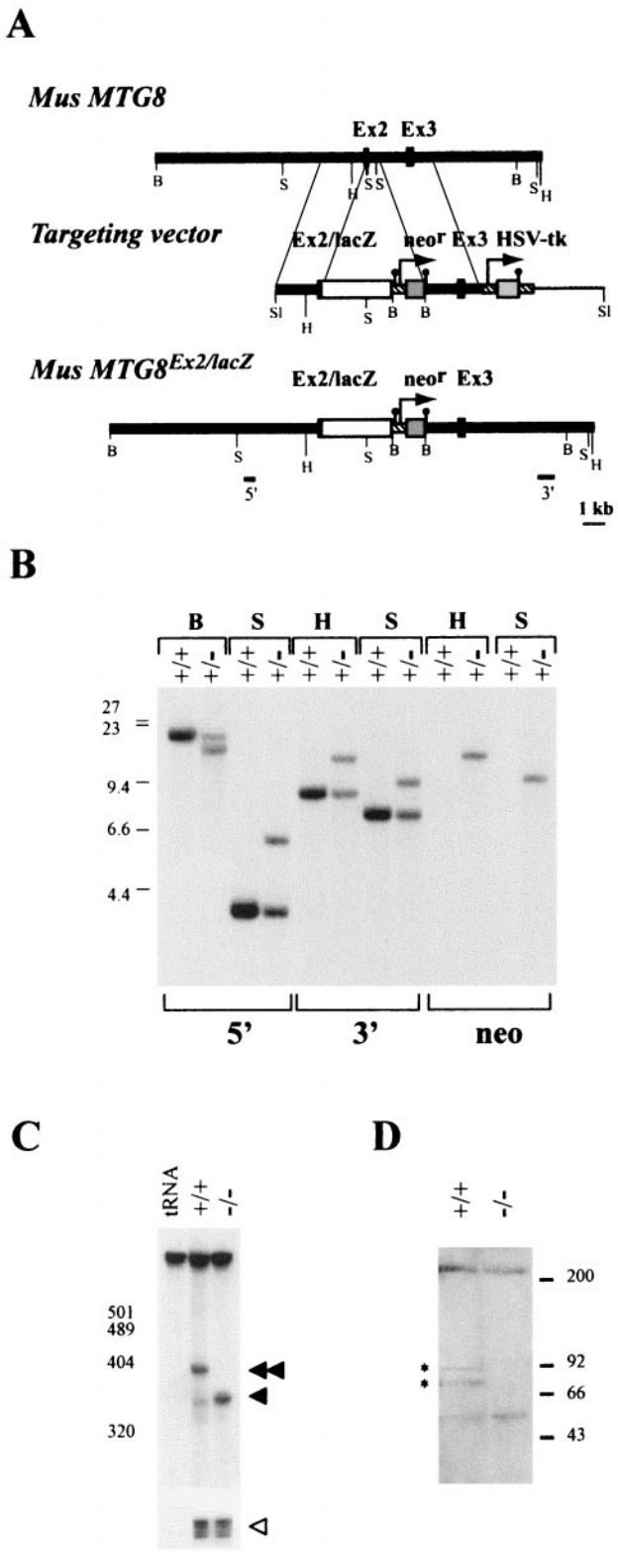


FIG. 1 Generation and expression of the *MTG8*$^{Ex2/lacZ}$ allele. (A) Diagram of the wt locus, the targeting vector and the mutant locus. Thick black line and boxes, murine *MTG8*; white box, *lacZ*; dark gray box, *neo*$^r$ gene; light gray box, *tk* gene; thick striped lines, promoters (arrows indicate transcriptional starts) and 3′ UTR [lollipop symbols indicate poly(A) signals]; thin line, pUC18. The 5′ and 3′ bars indicate the positions of the probes flanking the targeted region and used in the Southern analysis. Relevant restriction sites are represented by capital letters (B, *Bam*HI; H, *Hin*dIII; S, *Sst*I, Sl, *Sal*I). (B) Southern blotting analysis of wt (+/+) and *MTG8*$^{Ex2/lacZ}$-targeted (+/−) CCB ES cells. Restriction enzymes are as in panel A. The probes are described in Materials and Methods. The numbers on the left indicate the molecular size markers in kilobase pairs. (C) S1 protection analysis of brain RNA from wt (+/+) and *MTG8* exon 2-null (−/−) pups with a probe spanning *MTG8* exons 2 to 4 (Table 1). tRNA, negative control for probe hybridization. The top band corresponds to residual undigested full-length probe. The double filled arrows point to the band resulting from full protection of *MTG8* sequences; the single filled arrow points to the band resulting from protection of exons 3 and 4 only. For reference purposes, protection by an actin probe added to the same hybridization mixture is shown at the bottom (single open arrow). The numbers on the left indicate the molecular size markers in nucleotides. (D) Western blotting analysis of brain from wt (+/+) and *MTG8* exon 2-null (−/−) mice with an antiserum against the C-terminal domain of MTG8. No bands were visible with normal rabbit serum (data not shown). Asterisks mark species that are absent in the mutant. The numbers on the right indicate the molecular size markers in kilodaltons.

tal) stump was blind ended. On histopathological analysis, neither segment showed any significant anomaly, with the exception of a dilated vascular network, more prominent over the sigma-rectum, where microscopic examination occasionally revealed intraparietal and intraluminal hemorrhages (data not shown). While disjointed, the stumps were loosely held together by a short, fibrous, highly vascularized membrane in place of the mesentery. No gut structure was visible spanning the gap.

Genotyping showed the Δmidgut phenotype to occur nearly exclusively in homozygous mutant pups, at a frequency of ~25%. It can thus account for most of the increased perinatal mortality of this class. Much rarer cases were observed in heterozygotes (~1.3%), and none were seen in wt mice.

**Growth impairment in *MTG8* exon 2-targeted mice.** Of the offspring of heterozygous crosses surviving past the first 48 h, a number showed impaired growth, becoming progressively more marked during the subsequent 2 weeks. Typically, pups were 30 to 50% the size of normal littermates in weight, albeit well proportioned and normally active, except for the most extreme cases. Mortality was high. The few surviving mice gradually recovered with age after puberty, while remaining of below-average weight.

Nearly all affected mice were homozygous mutants. Conversely, all of the latter showed growth impairment. Thus, the phenotype was strongly associated with homozygosity for the *MTG8* exon 2-null allele.

Upon sacrifice, growth-impaired mice did not show any obvious anomaly outside the gastrointestinal tract. The intestine, while of reduced length compared to control littermates, was proportionate to the lower body weight. However, the gut histology was grossly abnormal, particularly at the level of the jejunum (Fig. 2C). The intestinal wall was thinner, largely due to a reduction in the length of the villi, which also looked highly disorganized, thicker, and fewer in numbers. Moreover, the lumen was often dilated, probably reflecting a reduced tone of the muscle layers.

In order to investigate whether the abnormal architecture was associated with changes in cellular differentiation, sections from pathological and normal guts were stained for gut cell

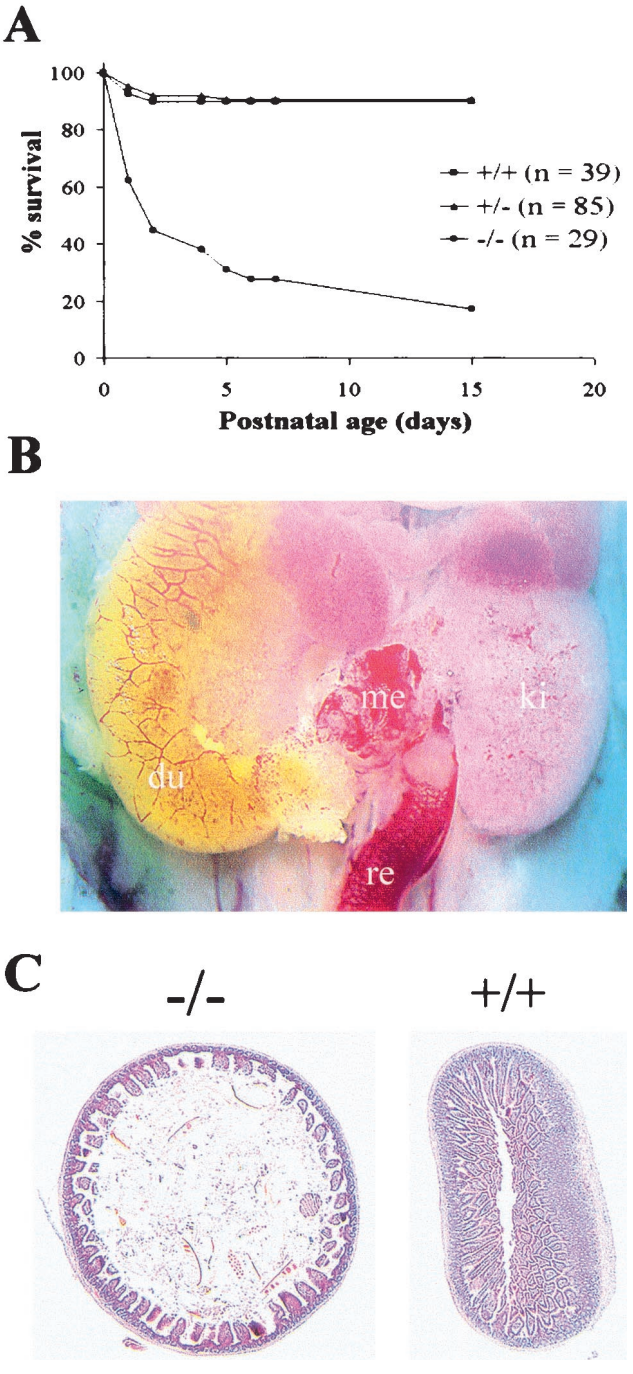


FIG. 2. (A) Viability of the offspring from crosses between *MTG8*$^{Ex2/lacZ}$ heterozygous mice. The cumulative percent survival over the first 2 weeks after birth of 153 newborn pups representing all accounted offspring of 17 matings is shown. All five *MTG8* exon 2-targeted homozygous mice surviving past day 15 were severely growth retarded. (B) ΔMidgut phenotype. An in situ view following sacrifice of a P0 homozygous mutant pup is shown. The defect extends from the distal portion of the duodenum to the rectum. The duodenal end is covered by an outgrowth of the mucosa, the rectal stump is surrounded by a prominent vascular network and the residual mesentery is hypervascularized. du, duodenum; ki, kidney; me, mesentery; re, rectum. (C) Abnormal gut structure in growth-impaired, *MTG8* exon 2-targeted mice. A low-power view of hematoxylin and eosin-stained jejunal sections from mutant (−/−) and control (+/+) P29 mice is shown. Note in the mutant the reduction in gut wall thickness due primarily to disorganization of the villi; note also the dilation of the lumen.

markers. Of the four main types of gut epithelial cells, enterocytes can be identified by the expression of sucrase-isomaltase and goblet and Paneth cells by a combination of Alcian blue and lectin UEAI staining. Contractile cells in the tunica muscularis, as well as in perivascular locations, express α-smooth muscle actin, and ENS cells express β-tubulin III. As shown in Fig. 3, all five cell types were present in homozygous mutant guts, in proportions and locations that were not significantly different from those of wt littermates.

The size of the intestinal villi results from the proliferative activity of cells in crypts. Quantitation of PCNA-positive, cycling cells in *MTG8* exon 2-targeted and wt littermates (Fig. 3) does not show any significant difference, indicating that the shorter villi in the mutants are not the result of decreased epithelial stem cell activity.

**Mouse *MTG8* is expressed in the mesoderm of the developing gut.** While *MTG8* has not been reported to be expressed in the adult gut, the phenotype of *MTG8* exon 2-targeted mutants suggested it plays a key role in the gastrointestinal system. In order to test this hypothesis, *MTG8* expression was studied during development, by staining heterozygous *MTG8*$^{Ex2/lacZ}$ embryos for β-galactosidase. Validation of the method was sought in preliminary experiments on adult tissues, in which the results obtained with the β-galactosidase stain were found to match faithfully those obtained by RNA analysis in wt mice (data not shown).

At the 26-somite stage, *MTG8* is clearly expressed throughout the primitive gut, albeit at the highest levels in the hindgut (Fig. 4, top panels). Most of the LacZ signal is localized outside the epithelial layer lining the gut lumen, i.e., in the mesodermally derived component.

This pattern becomes even more obvious at later stages. At E14.5 (Fig. 4, bottom panels), there is strong expression in the outermost gut tube layers and the contiguous mesentery, whereas almost no signal is detectable in the epithelium lining the lumen and in the subjacent lamina propria.

**Developmental origin of the gut phenotype in *MTG8* exon 2-targeted mice.** In order to define the developmental origin of the gut phenotype associated with the *MTG8* exon 2-null allele, embryos from heterozygous crosses were collected between E9.5 and E17.5, corresponding to the stages at which most of the critical gut morphogenetic events occur. Compared to wt littermates, no significant difference was observed up to E15.5 although, at the latter time point, the size of the umbilical hernia appeared to be somewhat smaller than in controls and the complexity of the midgut loops was reduced (data not shown). However, a disruption of the villi similar to, albeit less extensive than, that seen in postnatal cases was clearly apparent at E17.5 (Fig. 5). This was associated with persistence of the umbilical hernia, normally disappearing entirely by E16.5. Although preliminary, the data indicate that the requirement for wt MTG8 in the gut starts in the late stages of prenatal development.

**Expression of gut patterning factors in *MTG8* exon 2-targeted mutants.** Gut development is known to be controlled by a number of factors which, as in other systems, can be distinguished into two classes: signaling factors, mediating cellular interactions, and transcription factors, directly controlling gene activity. The former includes mesodermally derived Bmp4 and endodermally derived shh/ihh (39). Among the latter class, in

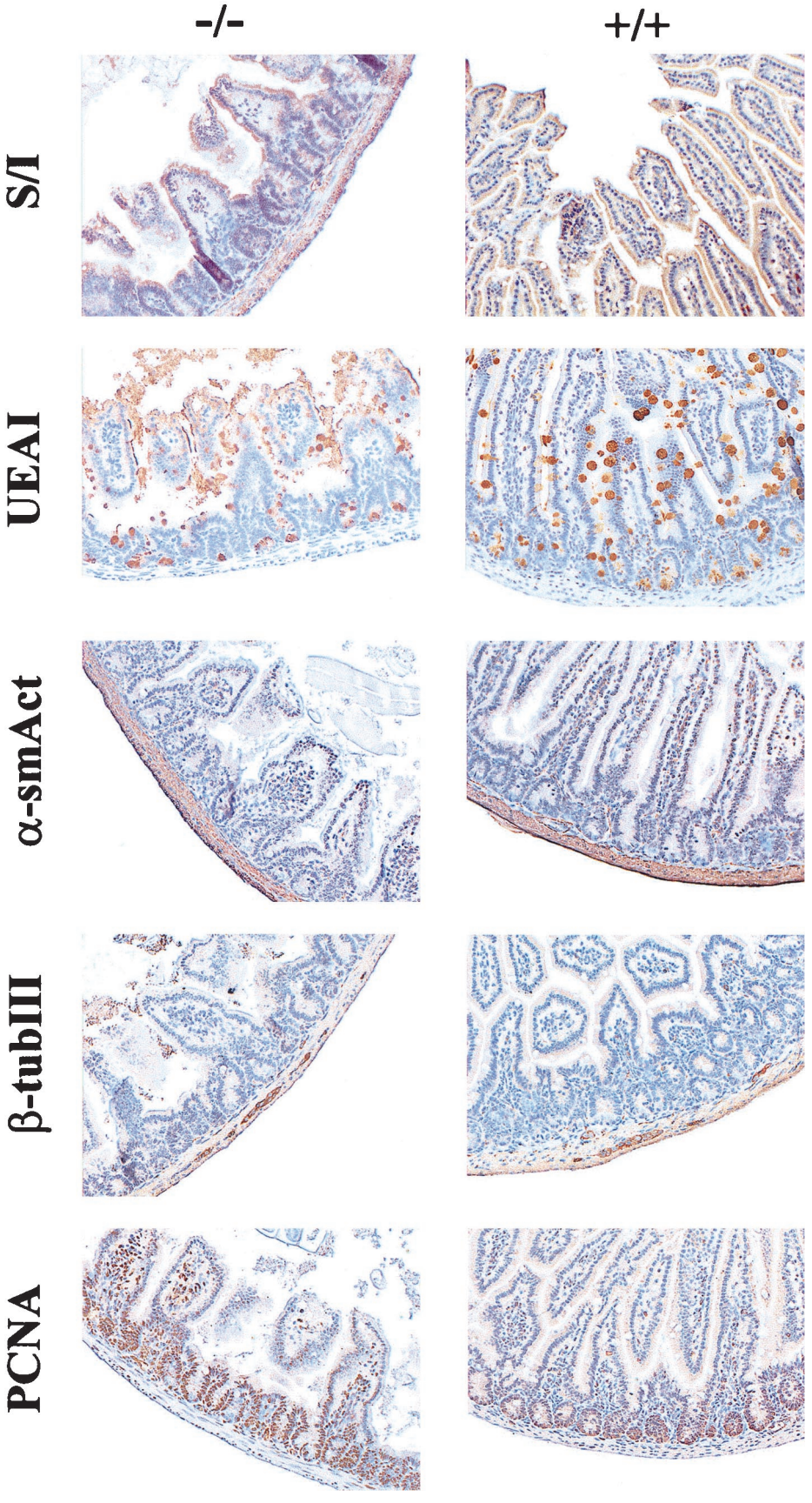
-/-
+/+
S/I
UEAI
α-smAct
β-tubIII
PCNA

addition to Hox gene products (Hoxd13), knockout experiments have revealed a crucial role for the *D. melanogaster* caudal homologue Cdx2 (encoded in the ParaHox cluster) (5), as well as for Fkh6 (belonging to the forkhead family) (13) and Nkx2-3 (a homeobox gene product) (25). Since *MTG8* is expressed in the mesoderm of the primitive gut and since its mutation has dramatic consequences on the gut structure, we sought to determine their relationship to other gut patterning factors by examining its expression in *MTG8* exon 2-targeted mutants. RNA was extracted from proximal and distal gut segments of growth-impaired $MTG8^{Ex2/lacZ}$-homozygous mice and wt littermates, and transcript levels were analyzed by nuclease protection. Representative results are shown in Fig. 6. Despite some occasional minor differences, there was no consistent change in RNA levels of Bmp2/4, Cdx1/2, Nkx2-3, or Fkh6 between the null mutant and the wt in either segment. Thus, the role of *MTG8* in the gut is not mediated through one of the already-identified gut patterning factors.

## DISCUSSION

In order to investigate the function of the *MTG8* locus, we generated a mutant allele, $MTG8^{Ex2/lacZ}$, in which part of exon 2 and of the downstream intron have been replaced by sequences encoding β-galactosidase and neomycin phosphotransferase. The sequence encoded by exon 2, spanning 46 amino acids, is very close to the proposed alternative amino termini. While alternative splicing has been observed both 5′ and 3′, exon 2 has never been found missing either from wt MTG8 transcripts (20, 40; Calabi, unpublished) or from runx1/MTG8 fusion transcripts arising from the t(8;21) of AML (30, 35). This suggests that this exon plays a crucial function, although it does not encode any of the four regions (NHR1 to -4) that are conserved among all MTG8-like polypeptides, and database searches have yet to reveal any significant homology.

Lack of MTG8 polypeptides carrying exon 2-encoded sequences results in high mortality, either perinatally or associated with significant growth impairment during the first 2 weeks of life. Most of the early mortality is due to a massive defect in the gastrointestinal tract. An abnormal gut structure is also found in growth-impaired mice and is a plausible cause of the latter phenotype, given its likely effects on the absorption of nutrients. As in other cases of gene targeting, variable phenotypic penetrance and/or expression may be explained by genetic heterogeneity within the strain resulting from targeting and may indicate the existence of interacting genetic factors. Moreover, a gene dosage effect is suggested by the occurrence of a similar phenotype in heterozygous mice, albeit at a much reduced frequency.

Our results indicate that *MTG8* has a crucial function in the gastrointestinal system. While no appreciable expression has been detected in the adult gut, our data show that the embryonic gut is, with the heart (data not shown), one of the main sites of expression at least from E9.5. The highest levels are found in the outer layers, in contrast to other factors so far found to be expressed in the developing gut, which are either endodermal (Cdx1 and -2, shh/ihh, Bmp2, and Tcf4) or primarily restricted to the subendodermal mesoderm (Nkx2-3, Fkh6, Gli1/Ptc, and Bmp4) (2, 13, 17, 25, 27). Intriguingly, the *Drosophila* homologue of *MTG8 (nervy)* was isolated as a downstream target of *Ubx* (9), which is known to play a role in gut patterning in the fruitfly (3). However, no phenotype is associated with *nervy* mutations, and the role of the latter in the fruitfly remains to be established, as is the potential existence of a *Hox-MTG8* pathway in higher organisms.

The Δmidgut phenotype shows some analogies to intestinal atresias in humans, which are generally believed to result from vascular accidents, although a genetic origin has been implicated in some cases (31). The extent of the defect largely coincides with the districts supplied by the superior mesenteric artery. Moreover, while the latter seems to be properly formed, there is vascular congestion over the proximal and particularly the distal gastrointestinal stumps, albeit with no evidence of necrosis. Unlike human cases, however, there is no proximal atresia, while a peculiar mucosal outgrowth extends from the duodenal end. There are no remnants of the missing gut segments, and the mesentery, albeit greatly shortened, shows no gaps. The contribution of *MTG8* mutations to gut defects in humans remains to be investigated.

The milder phenotype associated with the *MTG8* exon 2 knockout has some superficial analogies with those recently described in other mice with targeted disruption of genes involved in gut development. Both *Fkh6*- and *Nkx2-3*-null embryos show delayed formation and slower growth of villi (13, 25). In both cases the changes are apparent from the time of the initial transition from pseudostratified to columnar gut epithelium, coincide with alterations in the proliferative compartment, and correlate with a reduction in the levels of Bmp2 and -4 mRNA, suggesting that they are mediated via a common signaling pathway. In *Tcf4*- and *ihh*-null mice (17, 27), which die at or shortly after birth, there is a substantial decrease in the size of the villi associated with a reduction or, respectively, a nearly complete absence of proliferating stem cells. Similarly to these other null mutants, the milder gut phenotype of *MTG8* exon 2-targeted mice shows disorganization of the villi, which coexists with largely normal differentiation of gut cell lineages and is most pronounced in the proximal intestine (i.e., the jejunum). However, early midgut morphogenetic events (i.e., the formation of epithelial ridges) are not affected (data not shown), and cell proliferation is not reduced. Further proof that the *MTG8* function in gut development and/or differentiation is independent of previously identified pathways is provided by the analysis of patterns of

FIG. 3. Cell lineages and proliferation in the jejunum of growth-impaired *MTG8* exon 2-targeted mice. Jejunal sections from the mice shown in Fig. 2 were stained for markers of differentiated and proliferating cells. Sucrase-isomaltase (S/I) is a brush border enzyme characteristic of enterocytes; UEAI lectin (UEAI) binds to α-linked fucose residues in polysaccharides secreted by goblet and Paneth cells; α-smooth muscle actin (α-smAct) is present in the muscle layers of the gastrointestinal tract, as well as in vascular smooth muscle cells and myofibroblasts; β-tubulin III (β-tubIII) identifies ENS cells, and PCNA is an antigen associated with actively cycling cells. A positive reaction (brown color) was developed by the immunoperoxidase-diaminobenzidine technique, followed by counterstaining with Gill's hematoxylin. Despite the disruption of the gut architecture, the rates of cell differentiation and cell proliferation in the mutant are not significantly different from those in the control.

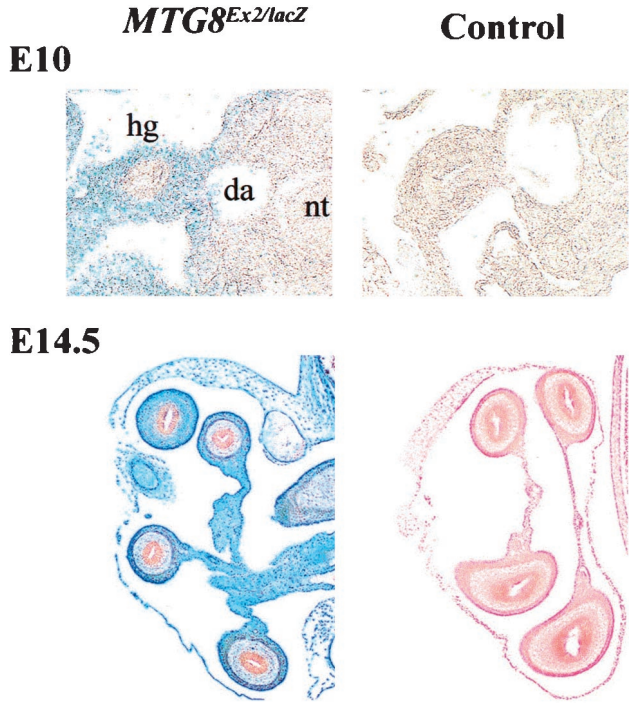


FIG. 4. *MTG8* expression in the embryonic gut. Transverse sections through $MTG8^{Ex2/lacZ}$-heterozygous and wt embryos at E10 and E14.5, stained for β-galactosidase activity as a proxy for *MTG8* expression, are shown. E14.5 sections were counterstained with eosin. *MTG8* is expressed in the mesodermally, rather than in the endodermally, derived tissue and becomes restricted, at the later time point, to the outermost gut layers. fg, foregut; hg, hindgut; da, dorsal aorta.

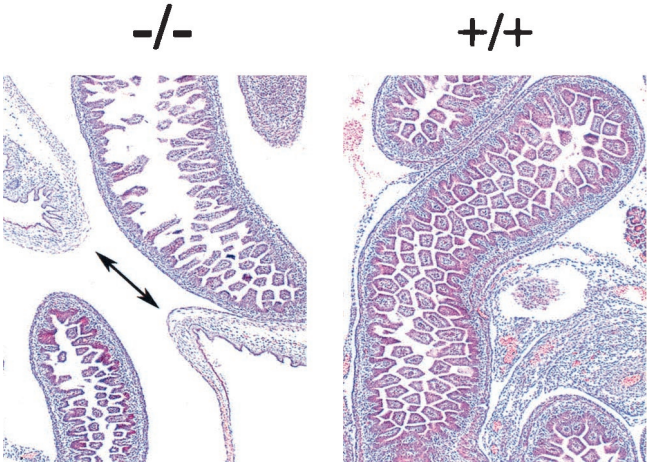


FIG. 5. Developmental origin of the gut phenotype in *MTG8* exon 2-targeted mice. Hematoxylin and eosin-stained transverse sections through the region of the umbilical hernia of *MTG8* exon 2-targeted (−/−) and control (+/+) E17.5 embryos are shown. In the former, the double-headed arrow indicates the communication between the abdominal cavity and the umbilical hernia, which is still prominent, whereas it has normally disappeared at this stage in control littermates.

gene expression in the mutants: Bmp2/4, Cdx1/2, Nkx2-3, and Fkh6 mRNA levels are essentially unchanged in the *MTG8* exon 2 knockout.

We hypothesize that the two distinct phenotypes of *MTG8* exon 2 mutant mice represent different degrees of severity of the same condition, resulting from the lack of a single *MTG8*-controlled function. Such function is unlikely to be required for primary gut morphogenesis, since the gut was fully formed in a majority of mutants, and no gut anomaly was found in homozygous mutant embryos up to E15.5. Primary canalization of the gut tube in the Δmidgut phenotype is also indicated by the finding of meconium in the rectal stump (data not shown) and by the absence of concomitant abdominal wall defects indicative of a failure in the process of embryonic folding or ventral midline fusion.

We suggest that *MTG8* is required for the maintenance of a normal gut structure from late embryonic development, since pathologic changes can be clearly detected in the mutants by E17.5. This function may be related to the blood supply of the midgut, leading in the most extreme cases to a complete regression (Δmidgut) and in less severe cases to dysplasia (causing malabsorption). Rescue of the latter phenotype may occur due to the postnatal triggering of compensatory mechanisms, similar to what has been reported in other knockouts. This hypothesis would be consistent with the localization of *MTG8* expression to the outermost layers of the gut, containing the main submucosal vascular plexuses.

In addition to the gastrointestinal defects, sterility was consistently observed in the few male null mutants surviving into adulthood. While the basis of this phenotype remains to be clarified, X-Gal staining in $MTG8^{Ex2/lacZ}$ heterozygotes shows *MTG8* to be mostly expressed by Leydig cells in the adult testis. This suggests that male sterility in homozygotes, despite apparently normal testis size and morphology, is due to hormonal insufficiency. Hind limb paresis and/or paralysis was rarely observed in adult mutant mice. By X-Gal staining in heterozygotes, we have been unable to detect *MTG8* expression in the spinal cord, peripheral nerves, or skeletal muscles, and the cause of this phenotype remains to be investigated. In contrast, insertional inactivation of *MTG8* exon 2 is phenotypically silent in the brain, lung, or heart, all major sites of expression. Histological examination has also so far failed to reveal any abnormality (data not shown). Thus, the function of *MTG8* in these organs is likely to be at least potentially redundant, and its absence may be compensated for by an increase in alternative isoforms and/or by *MTG8* paralogues.

Finally, our data do not support a role for *MTG8* in haemopoiesis. Upon X-Gal staining, no significant expression of the $MTG8^{Ex2/lacZ}$ allele was found either in embryos or in the main hemopoietic lineages of adult mice (data not shown). The bone marrow Ly-6A/$E^+$ subpopulation, containing hemopoietic stem cells, also scored negative. Moreover, no hemopoietic defect was observed in homozygous mutant mice. These data contrast with the report of *MTG8* expression in human $CD34^+$ cells (8). Apart from possible species-specific differences, the latter results may have rather been due to cross-reacting products encoded by *MTG8* paralogues, which are known to be expressed in hemopoietic cells (4, 7, 10). We conclude that the role (if any) of *MTG8* in leukemia may be at least partly related to its abnormal expression in hemopoietic precursors.

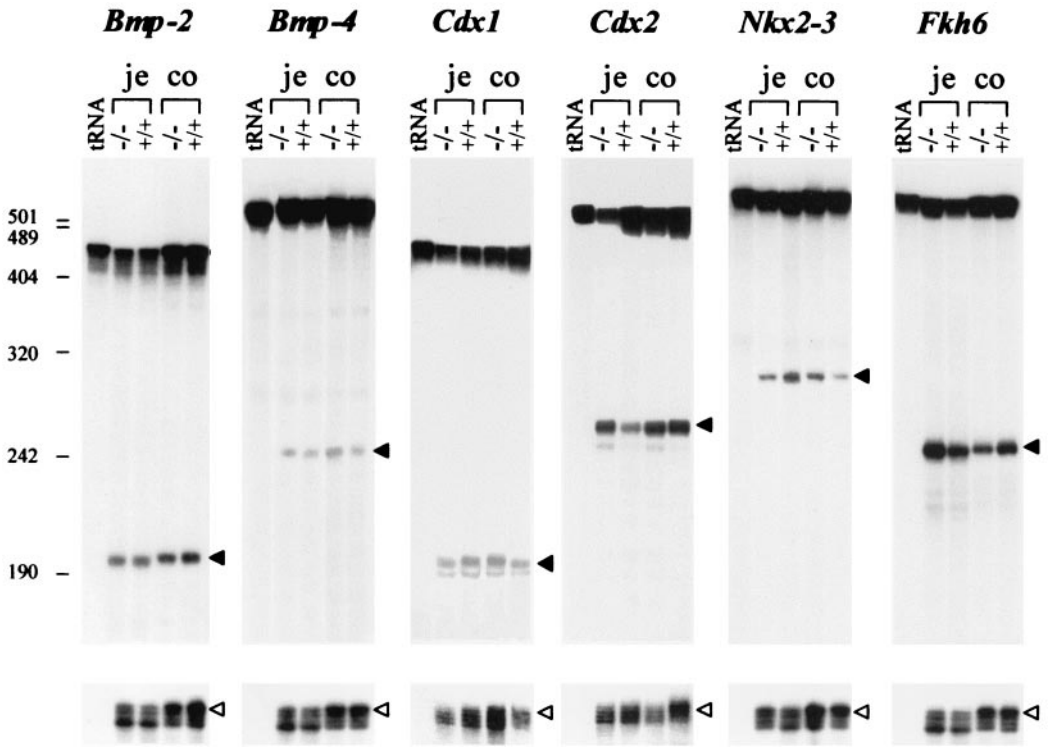


FIG. 6. Expression of gut morphogenetic factors in growth-impaired *MTG8* exon 2-targeted mice. S1 protection analysis of RNA from proximal (je) and distal (co) gut segments from a P7 *MTG8* exon 2-targeted homozygous pup (weight, 2.78 g) and a control (wt) littermate (weight, 5.98 g) was carried out. tRNA, negative control for probe hybridization. The probes are described in Table 1. The top band corresponds to residual undigested full-length probe. Filled arrows indicate the expected protected fragment for each probe. For reference purposes, protection by an actin probe added to the same hybridization mixture is shown at the bottom (white arrow). The numbers on the left indicate the molecular size markers in nucleotides. The apparent minor differences with some probes were inconsistent.

## ACKNOWLEDGMENTS

We are particularly grateful to Terence Rabbitts for constant encouragement and strategic advice. We also thank Vania Cilli for help in the isolation of mouse *MTG8* genomic clones, Dallas Swallow for the gift of the anti-human sucrase-isomaltase monoclonal antibody, Andy Copp and Patrizia Ferretti for comments, and the staff of the Royal Veterinary College, London, England, for expert mouse husbandry.

This work was supported by MRC PG9311737.

## REFERENCES

1. **Albright, S. R., and R. Tjian.** 2000. TAFs revisited: more data reveal new twists and confirm old ideas. Gene **242:**1–13.
2. **Beck, F., F. Tata, and K. Chawengsaksophak.** 2000. Homeobox genes and gut development. Bioessays **22:**431–441.
3. **Bienz, M.** 1994. Homeotic genes and positional signalling in the *Drosophila* viscera. Trends Genet. **10:**22–26.
4. **Calabi, F., and V. Cilli.** 1998. CBFA2T1, a gene rearranged in human leukemia, is a member of a multigene family. Genomics **52:**332–341.
5. **Chawengsaksophak, K., R. James, V. E. Hammond, F. Kontgen, and F. Beck.** 1997. Homeosis and intestinal tumours in Cdx2 mutant mice. Nature **386:** 84–87.
6. **Chomczynski, P., and N. Sacchi.** 1987. Single-step method of RNA isolation by acid guanidinium thiocyanate-phenol-chloroform extraction. Anal. Biochem. **162:**156–159.
7. **Davis, J. N., B. J. Williams, J. T. Herron, F. J. Galiano, and S. Meyers.** 1999. ETO-2, a new member of the ETO-family of nuclear proteins. Oncogene **18:**1375–1383.
8. **Erickson, P. F., G. Dessev, R. S. Lasher, G. Philips, M. Robinson, and H. A. Drabkin** 1996. ETO and AML1 phosphoproteins are expressed in $CD34^+$ hematopoietic progenitors—implications for t(8;21) leukemogenesis and monitoring residual disease. Blood **88:**1813–1823.
9. **Feinstein, P. G., K. Kornfeld, D. S. Hogness, and R. S. Mann.** 1995. Identification of homeotic target genes in *Drosophila melanogaster* including nervy, a protooncogene homolog. Genetics **140:**573–586.
10. **Fracchiolla, N. S., G. Colombo, P. Finelli, A. T. Maiolo, and A. Neri.** 1998. EHT, a new member of the MTG8/ETO gene family, maps on 20q11 region and is deleted in acute myeloid leukemias. Blood **92:**3481–3484.
11. **Gelmetti, V., J. S. Zhang, M. Fanelli, S. Minucci, P. G. Pelicci, and M. A. Lazar.** 1998. Aberrant recruitment of the nuclear receptor corepressor-histone deacetylase complex by the acute myeloid leukemia fusion partner ETO. Mol. Cell. Biol. **18:**7185–7191.
12. **Green, F. R., P. Greenwell, L. Dickson, B. Griffiths, J. Noades, and D. M. Swallow.** 1988. Expression of the ABH, Lewis and related antigens on the glycoproteins of the jejunal brush border, p. 119–153. *In* J. R. Harris (ed.), Subcellular biochemistry, vol. 12. Plenum Publishing, New York, N.Y.
13. **Kaestner, K. H., D. G. Silberg, P. G. Traber, and G. Schutz,** 1997. The mesenchymal winged helix transcription factor Fkh6 is required for the control of gastrointestinal proliferation and differentiation. Genes Dev. **11:** 1583–1595.
14. **Kagoshima, H., K. Shigesada, M. Satake, Y. Ito, H. Miyoshi, M. Ohki, M. Pepling, and P. Gergen.** 1993. The runt domain identifies a new family of heteromeric transcriptional regulators. Trends Genet. **9:**338–341.
15. **Kitabayashi, I., K. Ida, F. Morohoshi, A. Yokoyama, N. Mitsuhashi, K. Shimizu, N. Nomura, Y. Hayashi, and M. Ohki.** 1998. The AML1-MTG8 leukemic fusion protein forms a complex with a novel member of the MTG8(ETO/CDR) family, MTGR1. Mol. Cell. Biol. **18:**846–858.
16. **Komori, T., H. Yagi, S. Nomura, A. Yamaguchi, K. Sasaki, K. Deguchi, Y. Shimizu, R. T. Bronson, Y. H. Gao, M. Inada, M. Sato, R. Okamoto, Y. Kitamura, S. Yoshiki, and T. Kishimoto.** 1997. Targeted disruption of CBFA1 results in a complete lack of bone formation owing to maturational arrest of osteoblasts. Cell **89:**755–764.
17. **Korinek, V., N. Barker, P. Moerer, E. van Donselaar, G. Huls, P. J. Peters, and H. Clevers** 1998. Depletion of epithelial stem-cell compartments in the small intestine of mice lacking Tcf-4. Nat. Genet. **19:**379–383.
18. **Le, X. F., D. Claxton, S. Kornblau, Y. H. Fan, Z. M. Mu, and K. S. Chang.** 1998. Characterization of the ETO and AML1-ETO proteins involved in the 8;21 translocation in acute myelogenous leukemia. Eur. J. Haematol. **60:** 217–225.
19. **Lutterbach, B., J. J. Westendorf, B. Linggi, A. Patten, M. Moniwa, J. R. Davie, K. D. Huynh, V. J. Bardwell, R. M. Lavinsky, M. G. Rosenfeld, C. Glass, E. Seto, and S. W. Hiebert.** 1998. ETO, a target of t(8;21) in acute

leukemia, interacts with the N-CoR and mSin3 corepressors. Mol. Cell. Biol. **18:**7176–7184.
20. **Miyoshi, H., T. Kozu, K. Shimizu, K. Enomoto, N. Maseki, Y. Kaneko, N. Kamada, and M. Ohki.** 1993. The t(8;21) translocation in acute myeloid-leukemia results in production of an AML1-MTG8 fusion transcript. EMBO J. **12:**2715–2721.
21. **Miyoshi, H., K. Shimizu, T. Kozu, N. Maseki, Y. Kaneko, and M. Ohki.** 1991. t(8;21) breakpoints on chromosome-21 in acute myeloid leukemia are clustered within a limited region of a single gene, AML1. Proc. Natl. Acad. Sci. USA **88:**10431–10434.
22. **Mundlos, S., F. Otto, C. Mundlos, J. B. Mulliken, A. S. Aylsworth, S. Albright, D. Lindhout, W. G. Cole, W. Henn, J. Knoll, M. J. Owen, R. Mertelsmann, B. U. Zabel, and B. R. Olsen.** 1997. Mutations involving the transcription factor CBFA1 cause cleidocranial dysplasia. Cell **89:**773–779.
23. **Okuda, T., J. Vandeursen, S. W. Hiebert, G. Grosveld, and J. R. Downing.** 1996. AML1, the target of multiple chromosomal translocations in human leukemia, is essential for normal fetal liver hematopoiesis. Cell **84:**321–330.
24. **Otto, F., A. P. Thornell, T. Crompton, A. Denzel, K. C. Gilmour, I. R. Rosewell, G. Stamp, R. Beddington, S. Mundlos, B. R. Olsen, P. B. Selby, and M. J. Owen.** 1997. CBFA1, a candidate gene for cleidocranial dysplasia syndrome, is essential for osteoblast differentiation and bone development. Cell **89:**765–771.
25. **Pabst, O., R. Zweigerdt, and H. H. Arnold.** 1999. Targeted disruption of the homeobox transcription factor Nkx2–3 in mice results in postnatal lethality and abnormal development of small intestine and spleen. Development **126:**2215–2225.
26. **Rabbitts, T. H.** 1999. Perspective: chromosomal translocations can affect genes controlling gene expression and differentiation—why are these functions targeted? J. Pathol. **187:**39–42.
27. **Ramalho-Santos, M., D. A. Melton, and A. P. McMahon.** 2000. Hedgehog signals regulate multiple aspects of gastrointestinal development. Development **127:**2763–2772.
28. **Sambrook, J., E. F. Fritsch, and T. Maniatis.** 1989. Molecular cloning: a laboratory manual, 2nd ed. Cold Spring Harbor Laboratory Press, New York, N.Y.
29. **Sanes, J. R., J. L. Rubenstein, and J. F. Nicolas.** 1986. Use of a recombinant retrovirus to study post-implantation cell lineage in mouse embryos. EMBO J. **5:**3133–3142.
30. **Saunders, M. J., K. Tobal, S. Keeney, and J. Yin.** 1996. Expression of diverse AML1/MTG8 transcripts is a consistent feature in acute myeloid-leukemia with t(8;21) irrespective of disease phase. Leukemia **10:**1139–1142.
31. **Skandalakis, J. E., S. W. Gray, R. Ricketts, and D. D. Richardson.** 1994. The small intestine, p. 200–212. *In* J. E. Skandalakis and S. W. Gray (ed.), Embryology for surgeons, 2nd ed. The Williams & Wilkins Co., Baltimore, Md.
32. **Song, W. J., M. G. Sullivan, R. D. Legare, S. Hutchings, X. Tan, D. Kufrin, J. Ratajczak, I. C. Resende, C. Haworth, R. Hock, M. Loh, C. Felix, D. C. Roy, L. Busque, D. Kurnit, C. Willman, A. M. Gewirtz, N. A. Speck, J. H. Bushweller, F. P. Li, K. Gardiner, M. Poncz, J. M. Maris, and D. G. Gilliland.** 1999. Haploinsufficiency of CBFA2 causes familial thrombocytopenia with propensity to develop acute myelogenous leukaemia. Nat. Genet. **23:**166–175.
33. **Speck, N. A., T. Stacy, Q. Wang, T. North, T. L. Gu, J. Miller, M. Binder, and M. MarinPadilla.** 1999. Core-binding factor: a central player in hematopoiesis and leukemia. Cancer Res. **59:**S1789–S1793.
34. **Thomas, K. R., and M. R. Capecchi.** 1987. Site-directed mutagenesis by gene targeting in mouse embryo-derived stem cells. Cell **51:**503–512.
35. **Tighe, J. E., and F. Calabi.** 1994. Alternative, out-of-frame runt/MTG8 transcripts are encoded by the derivative(8) chromosome in the t(8;21) of acute myeloid-leukemia M2. Blood **84:**2115–2121.
36. **Wang, J. X., T. Hoshino, R. L. Redner, S. Kajigaya, and J. M. Liu.** 1998. ETO, fusion partner in t(8;21) acute myeloid leukemia, represses transcription by interaction with the human N-CoR/mSin3/HDAC1 complex. Proc. Natl. Acad. Sci. USA **95:**10860–10865.
37. **Wang, Q., T. Stacy, M. Binder, M. Marinpadilla, A. H. Sharpe, and N. A. Speck.** 1996. Disruption of the CBFA2 gene causes necrosis and hemorrhaging in the central nervous system and blocks definitive hematopoiesis. Proc. Natl. Acad. Sci. USA **93:**3444–3449.
38. **Warren, A. J., W. H. Colledge, M. B. Carlton, M. J. Evans, A. J. Smith, and T. H. Rabbitts.** 1994. The oncogenic cysteine-rich LIM domain protein rbtn2 is essential for erythroid development. Cell **78:**45–57.
39. **Wells, J. M., and D. A. Melton.** 1999. Vertebrate endoderm development. Annu. Rev. Cell. Dev. Biol. **15:**393–410.
40. **Wolford, J. K., and M. Prochazka.** 1998. Structure and expression of the human MTG8/ETO gene. Gene **212:**103–109.